Comparison of Dark Current Random Telegraph Signals in Silicon and InSb-Based Photodetector Pixel Arrays

Clementine Durnez, Vincent Goiffon, *Senior Member, IEEE,* Cedric Virmontois, *Senior Member, IEEE,* Pierre Magnan, *Member, IEEE,* and Laurent Rubaldo

***Abstract*— In this work, the parasitic discrete fluctuation of dark current (dc) called random telegraph signal (RTS) is analyzed in image sensors based on two different semiconductor materials: InSb and silicon. The results show that this dc-RTS phenomenon exhibits similar characteristics on both technologies strongly suggesting a common physical origin. This conclusion is extended to InGaAs and HgCdTe (also referred to as MCT)-based image sensors by comparing the presented results to the existing literature.**

***Index Terms*— CMOS image sensors (CISs), dark current, detectors, fluctuations, image sensors, indium antimonide, infrared, InSb, random telegraph signal (RTS), silicon, solid-state image sensors.**

I. Introduction

IMAGE sensors are widely used in many imaging systems ranging from commercial to scientific applications. These imagers are manufactured using different technologies depending on the final use. For visible and near-infrared (NIR) imaging, silicon-based image sensors are generally preferred. On the contrary, other semiconductors such as InSb, for MidWavelength InfraRed (MWIR) application, InGaAs for Short-Wavelength InfraRed (SWIR) application, or HgCdTe (also referred to as mercury cadmium telluride or MCT) from NIR to Long-Wavelength InfraRed (LWIR) are used to detect infrared wavelengths.

As image sensor's sensitivity is continuously improving over the years, one parasitic phenomenon becomes the limiting parameter for a growing number of applications: the dark current random telegraph signal (dc-RTS). It corresponds to a background signal directly collected by the photodetector that switches randomly between discrete current levels. Consequently, it becomes difficult to subtract this unwanted contribution to the collected signal, because transitions appear randomly with time. This implies calibration challenges and errors in measurements, which are neither permanent nor predictable. In the literature, the origin of the dc-RTS phenomenon has already been discussed in many silicon-based image sensors [1]. It is commonly admitted that this signal is due to the variation of a center generation rate, but the reason for such variation is not well understood.

Two main explanations are generally proposed.

1) The modulation of the electron/hole pair generation rate of a generation center by another defect which would change its configuration by capturing and emitting carriers [2]–[4].
2) Metastable generation centers switching spontaneously between several possible configurations and without involving the trapping and emission of a charge carrier [5]–[8].

The purpose of this work is to discuss the observed dc-RTS signals in several materials. The objective is to analyze and compare them, in order to highlight possible similarities.

II. Experimental Details

This article presents the results of two comparative measurement campaigns: one on a silicon-based image sensor and the other on an InSb device. Both pixel arrays use a reverse-biased photodiode as a photodetector. The silicon-based imager is a front-side illuminated CMOS active pixel sensor, also called a CMOS image sensor (CIS). It has been manufactured using a commercial 180-nm CIS process and is made of 512 × 512 pixels with a 7-μm pitch. Each pixel is composed of four transistors and a pinned photodiode (PPD) [9] depicted in Fig. 1. In the studied pixel array, the transfer gate (TG) is biased to 0 V when it is turned off and its channel cannot be fully accumulated. For this particular study, a subset of 100 000 pixels with the same design has been used. Various measurements were performed at several temperatures between 2 °C and 22 °C.

For each temperature, 10 000 frames were acquired with an integration time of 0.2, 0.5, or 1 s. As observed in infrared

The review of this article was arranged by Editor L. Pancheri. *(Corresponding author: Vincent Goiffon.)*

Clementine Durnez, Vincent Goiffon, and Pierre Magnan are with ISAE-SUPAERO, Université de Toulouse, F-31055 Toulouse, France (e-mail: vincent.goiffon@isae.fr).

Cedric Virmontois is with the CNES, 31401 Toulouse, France.

Laurent Rubaldo is with Lynred, 38113 Veurey-Voroize, France.

Digital Object Identifier 10.1109/TED.2020.3022336

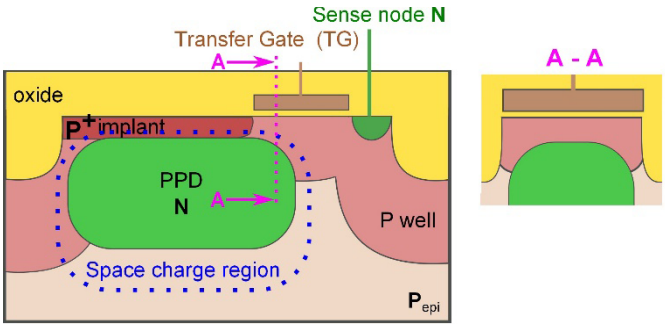

Fig. 1. Cross section of the 4T PPD. The P implants isolate the SCR from the oxide.

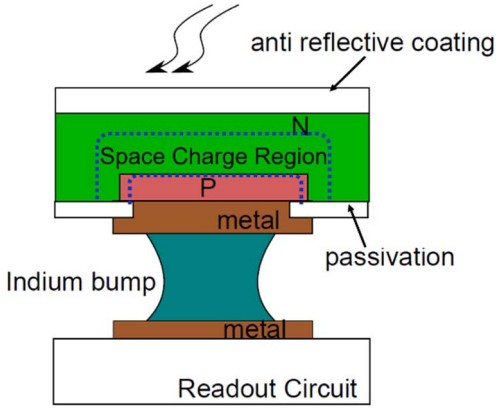

Fig. 2. Cross section of the InSb photodiode.

sensors, nonirradiated silicon pixel arrays have dc-RTS pixels [10] but only a small amount. In order to obtain more statistics for this comparison, the CIS was irradiated with 10-keV X-rays up to 10 krad. It has already been demonstrated [11] that this type of irradiation increases significantly the number of RTS pixels without changing their nature. In these conditions, most of the observed RTS are either bilevel RTS or multilevel RTS caused by the superimposition of two or more RTS centers in the same pixel.

The InSb imager sensor uses a direct injection readout circuit. It consists of 320 × 256 pixels and operates at cryogenic temperature. The cross section of the reverse-biased InSb photodiode is shown in Fig. 2. Several measurements were done at several temperatures around 80 K. As for the silicon detector studied here, the wide majority of observed RTS in this unirradiated InSb pixel array are two-level RTS or a sum of two-level RTS.

The results on InGaAs and HgCdTe materials that are presented in this article are based on the literature.

III. Experimental Results: Mean Dark Current

The dark current is the remaining signal that is collected when there is no incident photon. This parasitic signal originates in the thermally stimulated generation of electron–hole (e–h) pairs. Intrinsic defects which introduce energy levels within the bandgap can assist this phenomenon.

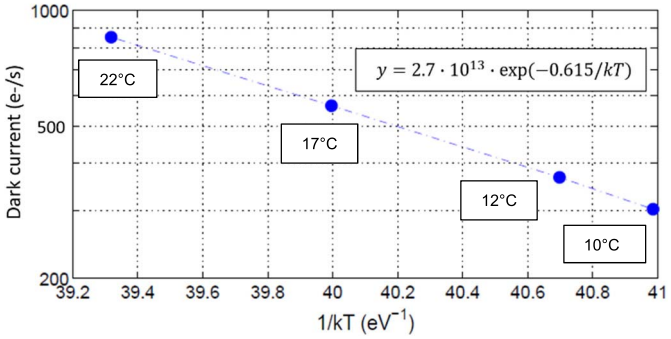

Fig. 3. Mean dark current evolution with $1/kT$ of the silicon detector: extraction of the mean dark current activation energy.

Two different mechanisms at the origin of dark current are considered in the semiconductor materials of interest for this study [12].

1) The Shockley–Read–Hall (SRH) generation current which corresponds to the e–h pair generation in the depletion region, also called space charge region (SCR).
2) The diffusion current which corresponds to the e–h pair generation outside the SCR. Those carriers are then collected by the diffusion process.

A. Mean Dark Current in Silicon-Based Imagers

Because of their high sensitivity, low noise, and ultralow dark current, 4T PPD CIS represents the main silicon image sensor technology today. Fig. 3 shows the mean dark current observed as a function of the temperature of the studied 4T PPD pixels (unirradiated). In this case, the TG is depleted and the PPD depletion region reaches the oxide interfaces in the TG vicinity. It can be seen that the trend of dark current with temperature is exponential, following an Arrhenius law. The slope allows the extraction of an activation energy, which corresponds to the half of the silicon bandgap (the measured value, 0.62 eV, is slightly higher than the midgap value, 0.56 eV, because the variation with the temperature of the exponential prefactor [12] is not taken into account in the calculation). Such evolution with temperature suggests that the underlying mechanism is the SRH generation inside the SCR due to defects with energy levels close to midgap [12]. On the contrary, when the TG is accumulated, the SCR narrows, and the mean dark current activation energy becomes more important (around the full bandgap value: 1.12 eV as shown experimentally and discussed in detail in [13] and [14]). This reveals that when the depletion region is not reaching any oxide, the diffusion current dominates. It also shows that in nonirradiated high-quality silicon wafers, the density of bulk defects with energy levels close to midgap is low enough to be hidden by the diffusion current mechanism. For the same reason, when the TG is properly accumulated, very few RTS pixels can be seen in such devices [10].

B. Mean Dark Current in InSb-Based Imagers

InSb imagers are used to detect MWIR wavelengths. The bandgap is 0.23 eV at 80 K. The narrow bandgap, the high

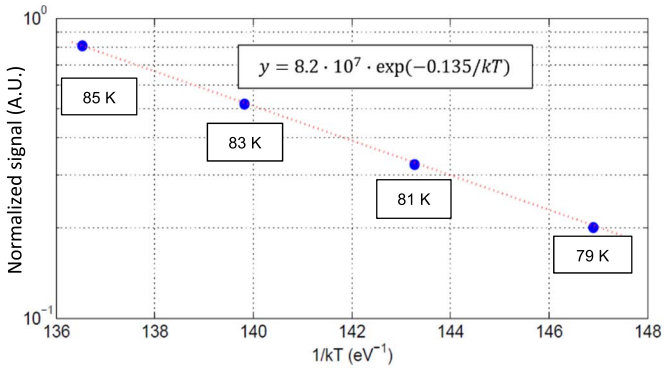

Fig. 4. Mean dark current evolution with $1/kT$ of the InSb detector: extraction of mean dark current activation energy. A.U. stands for arbitrary unit.

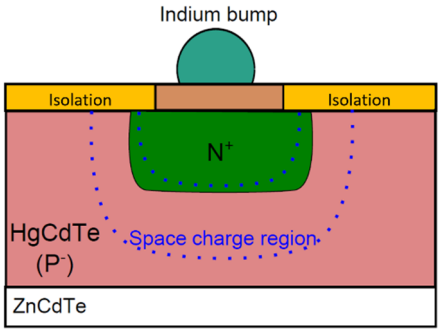

Fig. 5. Cross section of an HgCdTe-based photodiode.

carrier mobility, and the low life time of minority carrier due to defects imply a huge dark current at room temperature and necessitate operating the detector at cryogenic temperatures.

Fig. 4 shows the mean dark current as a function of the temperature measured on the studied InSb detector. The slope gives an activation energy close to 0.135 eV. As for silicon, this value is approximately half of the bandgap width (slightly higher for the same reasons as for silicon), which points to a SRH generation mechanism inside the SCR. This can be explained by the fact that in the InSb photodetector, the depletion region reaches the passivation oxide interface (on the side of the P-doped region in Fig. 2) that is rich in interface defects (and thus midgap generation centers). Such conclusion agrees well with [15] that demonstrates that the diffusion current empirical model from [16] does not match the observed behavior.

C. Mean Dark Current in HgCdTe-Based Imagers

Fig. 5 shows a HgCdTe photodiode cross section with a ZnCdTe substrate. It depicts an intrinsic n-on-p legacy technology, doped with mercury vacancy and boron implantation. CdTe/ZnS is used for passivation. The bandgap of HgCdTe can vary from 0 to 1.5 eV, depending on the alloy used, that is, the cadmium stoichiometry.

In the literature, dark current studies for P on N technology [17], [18] focus on two types of infrared bands: MWIR blue ($\lambda = 4.2$ μm at 150 K and bandgap of 0.3 eV) and

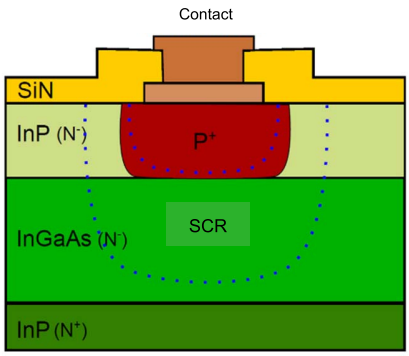

Fig. 6. Cross section of an InGaAs-based photodiode. SCR stands for space charge region.

MWIR red ($\lambda = 5.3$ μm at 130 K and bandgap of 0.23 eV). The temperature range used in these studies is [130, 180 K].

In both cases, the mean activation energy for dark current is around the value of the full bandgap. This reveals that on the contrary to InSb imagers, the mean dark current seems to be dominated by the diffusion mechanism. Moreover, the empirical diffusion current model from [16] applies well to HgCdTe photodiodes. It can also be noticed that for this type of photosensitive elements the passivation is made without an oxide thus reducing the number of interface-related defects in the depletion region. This most likely explains why the diffusion current contribution dominates as in silicon CIS pixels when the oxide interfaces are passivated by accumulating the TG. Finally, it can be concluded that all these observations support the idea that dark current in HgCdTe-based image sensors is dominated by the diffusion mechanism in the studied temperature range (130–180 K).

D. Dark Current in InGaAs-Based Imagers

Fig. 6 shows the cross section of an InGaAs photodiode. Zinc is used for the P doping [19]. The bandgap is 0.73 eV wide and thus this technology can be used at temperatures higher than cryogenic temperature, which makes it an attractive infrared detector technology. It has been clearly demonstrated in the literature that InGaAs photodiode dark current is dominated by the diffusion mechanism [19]–[21], as in silicon PPD CIS with the TG accumulated and as in HgCdTe devices. As mentioned for MCT in the previous section, it can be noticed that the passivation layer in the investigated InGaAs photodiodes is not an oxide, which prevents here again the creation of midgap interface SRH generation centers.

IV. Experimental Results: Dark Current RTS

In order to detect RTS pixels, several thousands of images are acquired, and then processed. An automatic tool [22] based on a simple edge detection technique is used to extract the population of RTS pixels in the image sensor.

A. Influence of the Illumination

The RTS signal studied here is assumed to come from a fluctuation of the dark current. This seems obvious in

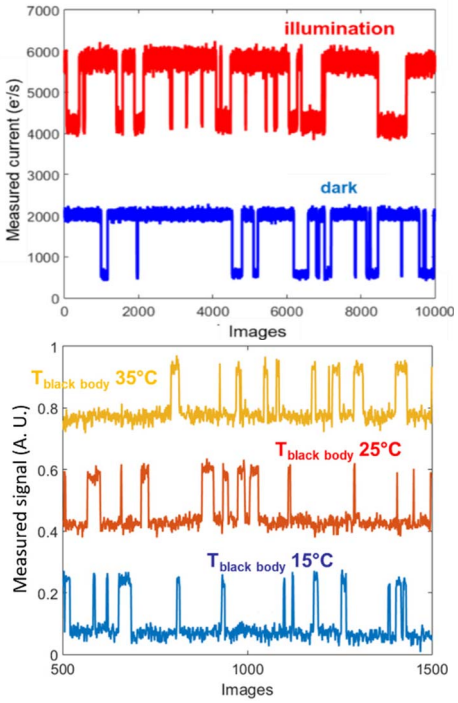

Fig. 7. Influence of illumination on RTS. A silicon detector is used at the top (at 22 °C) with a halogen lamp to illuminate the sensor. At the bottom, an InSb detector is used with a blackbody whose temperature is varied to modify the illumination level. A.U. stands for arbitrary unit.

silicon detector studies where all the measurements are performed in the dark (without illumination) but it may not be that clear when characterizing RTS in infrared detectors where a background illumination is almost always required to perform the measurement. Hence, this section aims at clarifying the influence of illumination on the studied RTS phenomenon.

Fig. 7 presents the signal of one pixel at different illumination conditions for a silicon detector at the top, and an InSb imager at the bottom. In both cases, it can be seen that the main RTS characteristics (number of levels, amplitude, and time constants) remain the same. The only changes are the offset variation due to the change in illumination and the background noise increase which corresponds to the addition of the photon shot noise. It can thus be inferred that the studied RTS signal does not come from the illumination and is not influenced by it. It confirms that the studied phenomenon is coming from the dark signal of the detectors.

B. Influence of the Integration Time

Figs. 8 and 9 show the evolution of one RTS signal at several integration times for the studied silicon imager and the studied InSb detector, respectively. For the silicon-based image sensor, it can be seen that there is a direct influence of the integration time on the amplitude, but not on the time constants nor on the number of levels. This behavior was already reported in [23]. It can be observed that the amplitude is proportional to the integration time. Thus, it can be deduced that the mechanism responsible for RTS signals is located in the photodiode because the integration time corresponds to the

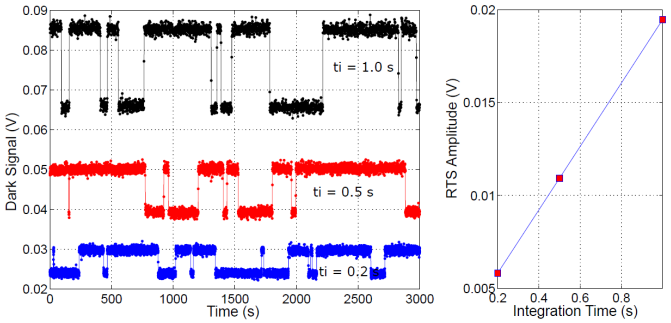

Fig. 8. RTS amplitude as a function of integration time for one pixel of the silicon-based imager at 22 °C. The RTS signal is shown on the left. The RTS amplitude evolution as a function of integration time is displayed on the right.

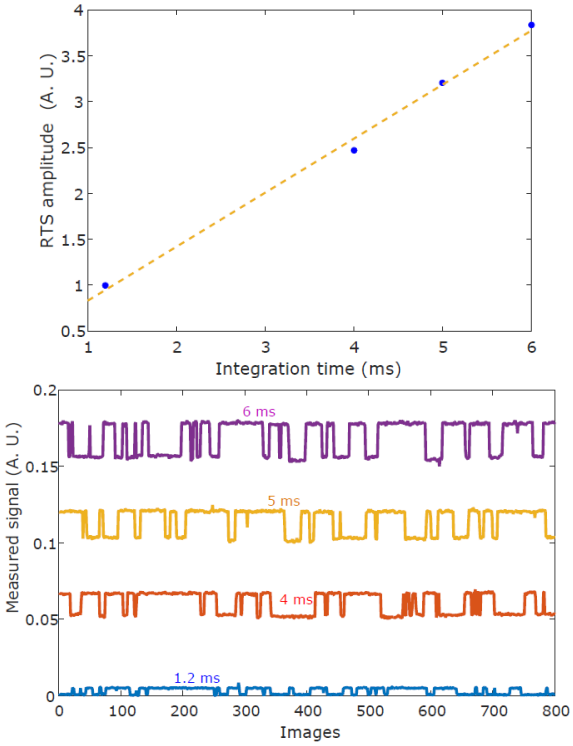

Fig. 9. RTS amplitude as a function of integration time for one pixel of the InSb-based imager at 80 K. (Top) RTS amplitude as a function of integration time. (Bottom) Temporal RTS trace. A.U. stands for arbitrary unit.

charge collection time while the transfer and readout durations stay constant whatever the exposure time.

Regarding the InSb-based imager, the same behavior is observed in Fig. 9. The amplitude appears proportional to the integration time. Here again, the time constants and the number of levels do not change when the integration time increases. Consequently, it can be concluded that the studied RTS phenomenon also originates from the photodiode dark current in InSb-based detectors.

C. Statistical Analysis of the RTS Amplitudes

The extraction of all RTS pixels from the image sensors allows performing statistical analysis on the main parameters, such as the RTS amplitude. Fig. 10 shows the histogram of

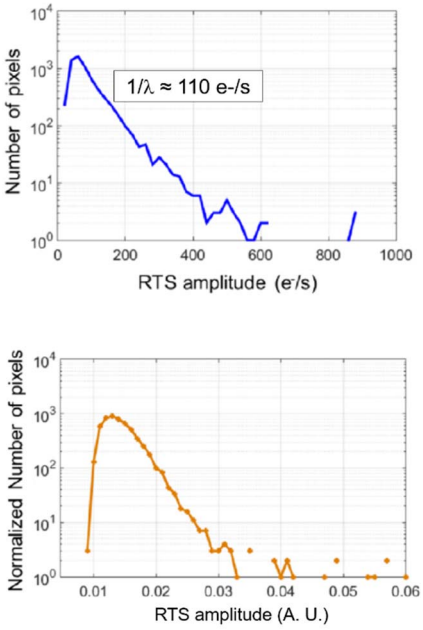

Fig. 10. Distributions of dc-RTS amplitudes for silicon at 22 °C (at the top for ≈6400 detected RTS pixels) and InSb at 80 K (at the bottom for ≈5400 detected RTS pixels).

the amplitudes for the case of the silicon detector at the top and the InSb image sensor at the bottom. The distribution shape is comparable in both cases. Above a current value corresponding to the detection threshold, the distributions decrease by following an exponential law characterized by

$$f(x) = K \times \exp(-\lambda \times x). \tag{1}$$

In these semilogarithmic plots, this exponential decrease appears as a straight line and its slope gives the parameter λ. It is worth mentioning that $1/\lambda$ is also the mean value of the exponential distribution. For the silicon imager, the slope of the distribution gives a value $1/\lambda \approx 110$ e^-/s at 22 °C. This value has been confirmed several times in the literature for dc-RTS induced by oxide defects in silicon [23], [24].

As mentioned above, the decrease of the number of pixel number at low amplitude is due to the detection limit. Indeed, as noise becomes predominant for these low amplitudes, it becomes difficult to detect RTS signals and the number of detected RTS pixels is lower than reality. Moreover, in the literature [24], such exponential distribution of amplitudes has also been observed for HgCdTe and InGaAs image sensors. The slope of the exponential curve gave $1/\lambda$ values around 210 e^-/s at 200 K for HgCdTe detector and 250 ke^-/s at 293 K for InGaAs-based photodiodes. Finally, since the reported RTS amplitude distribution shapes are the same for these four considered semiconductor materials, this analysis suggests that the underlying mechanism responsible for RTS could be the same for these different detectors technologies.

D. Temperature Dependence

The RTS phenomenon is thermally activated and the behavior of amplitudes with temperature has been reported

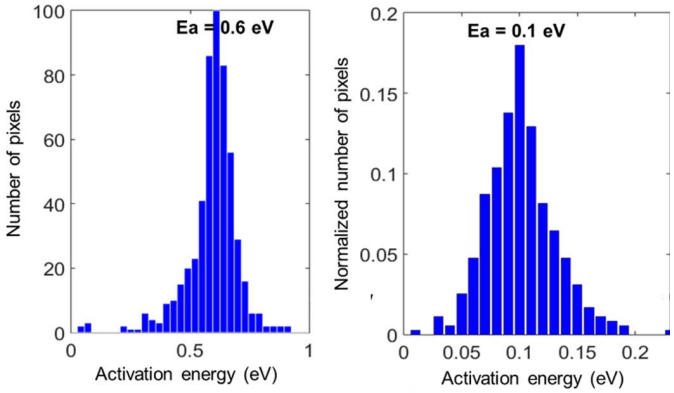

Fig. 11. Histogram of RTS amplitude activation energies on ≈500 RTS pixels for on the (left) silicon and (right) InSb.

in many articles [5], [6], [25]–[28], but mostly on silicon detectors.

Fig. 11 presents the histograms of the amplitude activation energies extracted from the population of RTS pixels which parameters could be accurately followed over the chosen temperature range (about 500 pixels for each detector) on the silicon-based imager (on the left) and the InSb one (on the right). A Gaussian-like shape is observed, with a peak at 0.6 eV for silicon (in agreement with the literature) and 0.1 eV for InSb. These values are not identical from an absolute point of view, but they are both close to half the bandgap width of their respective materials. This suggests an SRH generation mechanism from a depleted area for both materials. Moreover, in [24] and [26], the activation energy is 0.1 eV for a bandgap of 0.2 in HgCdTe. As for silicon and InSb, the underlying mechanism seems to be the *e–h* pair generation in depleted regions, even if the mean dark current is dominated by the diffusion contribution. Finally, in InGaAs [24], the value of the activation energy of RTS amplitude is about 0.44 eV for a bandgap of 0.73 eV. The ratio is slightly above 0.5, but still suggests an *e–h* pair generation mechanism in a depletion region.

V. Discussion

Table I recaps the characteristics of dark current and RTS amplitude for silicon and InSb detectors from this work alongside additional silicon, HgCdTe, and InGaAs data from the literature. For amplitude activation energies in silicon devices, many results can be found. Some of them show results below half the bandgap width. This is usually justified by the fact that a high electric field region exists in the studied device and that the apparent activation energy is lowered because of the electric field enhancement (EFE) phenomenon. However, the conclusion is always the same, even in the case of EFE: the silicon dc-RTS signal appears to originate from the SRH generation mechanism in depleted areas.

It has been shown in the previous sections that the mechanism responsible for dc-RTS appears similar for the four semiconductor materials studied in this work. It seems to be an SRH *e–h* pair generation process in depletion regions in every case, even if the mean background dark current is dominated

TABLE I
SUMMARY OF DARK CURRENT AND DC-RTS PROPERTIES OBSERVED FOR EACH TYPE OF SEMICONDUCTOR-BASED IMAGER[2]

	Si	InSb	HgCdTe	InGaAs
Bandgap Width Eg (eV)	1.12	0.23	0.2	0.73
Dark Current Activation Energy Ea_DC (eV)	4T PPD Depleted TG: 0.61 Accumulated TG: 1.1	0.1	0.2 [24]	-
Ea_DC/Eg	4T PPD Depleted TG: 0.5 Accumulated TG: 1	0.5	1	-
Dark Current Mechanism	4T PPD Depleted TG: Generation in SCR Accumulated TG: Diffusion	Generation in SCR	Diffusion from the quasi-neutral region	Diffusion from the quasi-neutral region
Mean RTS Amplitude $1/\lambda$ (e-/s)	110 for ionizing irradiation or without irradiation 1200 for non-ionizing irradiation at 295K [28]	-	210 at 200K [24]	250000 at 293K [24]
RTS Amplitude Activation Energy Ea_ampl (eV)	0.6 (0.57 [5], 0.58 [29], 0.75 [30], 0.44 [25],0.61 [6])	0.1	0.1 [24] [26]	0.44 [24]
Ea_ampl_RTS/Eg	0.5	0.45	0.5	0.6
Dark Current RTS Amplitude Mechanism	Generation in SCR	Generation in SCR	Generation in SCR	Generation in SCR

by a diffusion current.[1] Consequently, defects which induce this RTS phenomenon are most likely located inside the SCR.

As mentioned previously, two major hypotheses have emerged considering the origin of dc-RTS. The first one is the modulation of a generation center by a defect which would capture and emit single charges (as discussed in Section I). Since the results show that the RTS signal seems to originate from an SCR, it suggests that the modulator is also located inside the photodiode SCR. In such depletion region under nonequilibrium condition with $p\text{-}n \ll n_i^2$ electron (or hole) capture probability is extremely low and the generation mechanism (emission of both holes and electrons) dominates. Hence, a modulator defect that would change state by capturing and emitting a single type carrier (electron or hole) with a comparable probability in such depletion region is very unlikely.

However, as the defect or cluster of defects can be spread over a large distance, the modulator (or the modulating part of the large defect) could be located outside the SCR and influence the generation rate of the defect (or the part of the defect) inside the SCR. Moreover, as extended defects present very large sizes at atomic level, it is also possible that these defects create localized SCR themselves [31], which could also influence the generation rate of the RTS source.

The second hypothesis corresponds to the involvement of a metastable defect exhibiting several possible configurations without a change of charge state [2], [5]–[7]. The existence of such defects switching spontaneously between several geometrical configurations thanks to the interaction with a phonon has been discussed in several articles [8], [32]–[34]. This hypothesis seems compatible with the signatures observed for all the devices analyzed in this article.

VI. CONCLUSION

This work has compared photodiode dark current RTSs in several detector materials and technologies: silicon, InSb, HgCdTe, and InGaAs. The silicon and InSb results are coming from the experiment described in this article whereas the HgCdTe and InGaAs results are taken from the literature. It showed that the behavior is similar in all the cases: amplitude distributions, time constants, and temperature dependence have the same characteristics. Moreover, the origin of the mechanism seems to be the same in all the studied materials. Generation centers inside an SCR seem to be the source of the dark current RTS signals, whatever the origin of the main pedestal dark current (*e–h* pair generation in the depletion region or diffusion current). Consequently, the photodiode leakage/dark current RTS phenomenon does not seem dependent on the semiconductor material and conclusions regarding

[1]It is worth discussing further this latter particular situation. There are two typical situations where the main contribution to the mean dark current is the diffusion process and where SCR generation current RTS can be observed. First, when there is nearly no active defect in the SCR of the pixel array except a few damaged pixels exhibiting dc-RTS. This is for instance the case in accumulated PPD CIS pixel arrays exposed to nonuniform process damage or nonuniform radiation damage (e.g., case of neutron irradiations). In this case, the few damaged pixels exhibit a dark current dominated by SRH centers with an RTS behavior (and thus a midgap center signature) well above the background whereas the overall dark current of the whole pixel array remains dominated by the diffusion current. Second, when the dark current diffusion background is high enough to dominate the dark current pedestal of most of the pixels despite the significant density of defects in their SCR. This can happen for example in silicon pixel arrays (with depleted TG) at elevated temperature or in HgCdTe at operating temperature. In this situation, most of the observed dc-RTS amplitudes are small compared to the dark current pedestals and, even if numerous, they do not influence the overall mean dark current activation energy whereas the activation energy of their dc-RTS amplitude exhibits a midgap signature.

[2]The parameters listed in this table are assumed to be independent of pixel design, pixel dimensions, and manufacturing process. Absolute mean dark current values are not given here because they depend directly on pixel dimensions, pixel design, and process quality.

dark current RTS obtained on a given semiconductor material are probably applicable to the other detector technologies.

Acknowledgment

The authors would like to thank the ISAE-SUPAERO Image Sensor Team and Lynred's team for their help, especially Alexandre Le Roch, Federico Pace, Jean-Marc Belloir, Alice Pelamatti, Jean-Baptiste Lincelles, Alexandre Brunner, Rachid Taalat, and Pierre Guinedor for their help in the data analysis.

References

[1] E. Simoen and C. L. Claeys, *Random Telegraph Signals in Semiconductor Devices*. Bristol, U.K.: IOP, 2016.

[2] D. Pogány, J. A. Chroboczek, and G. Ghibaudo, "Random telegraph signal noise mechanisms in reverse base current of hot carrier-degraded submicron bipolar transistors: Effect of carrier trapping during stress on noise characteristics," *J. Appl. Phys.*, vol. 89, no. 7, pp. 4049–4058, Apr. 2001.

[3] A. Brunner, "Etude des bruits basse fréquence dans les détecteurs infrarouge quantiques refroidis à base de HgCdTe," Ph.D. dissertation, Univ. Grenoble Alpes, Saint-Martin-d'Hères, France, 2015.

[4] S. T. Hsu, R. J. Whittier, and C. A. Mead, "Physical model for burst noise in semiconductor devices," *Solid-State Electron.*, vol. 13, no. 7, pp. 1055–1071, Jul. 1970.

[5] I. H. Hopkins and G. R. Hopkinson, "Random telegraph signals from proton-irradiated CCDs," *IEEE Trans. Nucl. Sci.*, vol. 40, no. 6, pp. 1567–1574, Dec. 1993.

[6] J. Bogaerts, B. Dierickx, and R. Mertens, "Random telegraph signals in a radiation-hardened CMOS active pixel sensor," *IEEE Trans. Nucl. Sci.*, vol. 49, no. 1, pp. 249–257, Feb. 2002.

[7] C. Durnez, V. Goiffon, C. Virmontois, J.-M. Belloir, P. Magnan, and L. Rubaldo, "In-depth analysis on radiation induced multi-level dark current random telegraph signal in silicon solid state image sensors," *IEEE Trans. Nucl. Sci.*, vol. 64, no. 1, pp. 19–26, Jan. 2017.

[8] V. Goiffon *et al.*, "Radiation-induced variable retention time in dynamic random access memories," *IEEE Trans. Nucl. Sci.*, vol. 67, no. 1, pp. 234–244, Jan. 2020.

[9] E. R. Fossum and D. B. Hondongwa, "A review of the pinned photodiode for CCD and CMOS image sensors," *IEEE J. Electron Devices Soc.*, vol. 2, no. 3, pp. 33–43, May 2014.

[10] V. Goiffon, C. Virmontois, and P. Magnan, "Investigation of dark current random telegraph signal in pinned photodiode CMOS image sensors," in *IEDM Tech. Dig.*, Washington, DC, USA, Dec. 2011, pp. 8.4.1–8.4.4.

[11] C. Durnez *et al.*, "Total ionizing dose radiation-induced dark current random telegraph signal in pinned photodiode CMOS image sensors," *IEEE Trans. Nucl. Sci.*, vol. 65, no. 1, pp. 92–100, Jan. 2018.

[12] A. S. Grove, M. de Brébisson, J. Encinas, and J. Thiré, *Physics and Technology of Semiconductor Devices*. Hoboken, NJ, USA: Wiley, 1967.

[13] V. Goiffon *et al.*, "Radiation effects in pinned photodiode CMOS image sensors: Pixel performance degradation due to total ionizing dose," *IEEE Trans. Nucl. Sci.*, vol. 59, no. 6, pp. 2878–2887, Dec. 2012.

[14] D. McGrath, S. Tobin, V. Goiffon, P. Magnan, and A. Le Roch, "Dark current limiting mechanisms in CMOS image sensors," *Proc. Electron. Imag.*, vol. 2018, no. 11, pp. 354-1–354-8, Jan. 2018.

[15] F. K. Hopkins and J. T. Boyd, "Dark current analysis of InSb photodiodes," *Infr. Phys.*, vol. 24, no. 4, pp. 391–395, Jul. 1984.

[16] W. E. Tennant, D. Lee, M. Zandian, E. Piquette, and M. Carmody, "MBE HgCdTe technology: A very general solution to IR detection, described by 'rule 07', a very convenient heuristic," *J. Electron. Mater.*, vol. 37, no. 9, pp. 1406–1410, Sep. 2008.

[17] L. Rubaldo *et al.*, "State of the art HOT performances for sofradir II-VI extrinsic technologies," *Proc. SPIE*, vol. 9819, pp. 9819–9842, May 2016.

[18] J. W. Beletic *et al.*, "Teledyne imaging sensors: Infrared imaging technologies for astronomy and civil space," *Proc. SPIE*, vol. 7021, no. 2, 2008, Art. no. 70210H.

[19] J.-L. Reverchon, "High dynamic solutions for short-wavelength infrared imaging based on InGaAs," *Opt. Eng.*, vol. 50, no. 6, Jun. 2011, Art. no. 061014.

[20] J. Boisvert, T. Isshiki, R. Sudharsanan, P. Yuan, and P. McDonald, "Performance of very low dark current SWIR PIN arrays," *Proc. SPIE*, vol. 6940, May 2008, Art. no. 69400L.

[21] A. Rouvié *et al.*, "InGaAs focal plane array developments at III-V lab," in *Proc. SPIE*, vol. 8353, May 2012, Art. no. 835308.

[22] V. Goiffon, G. R. Hopkinson, P. Magnan, F. Bernard, G. Rolland, and O. Saint-Pe, "Multilevel RTS in proton irradiated CMOS image sensors manufactured in a deep submicron technology," *IEEE Trans. Nucl. Sci.*, vol. 56, no. 4, pp. 2132–2141, Aug. 2009.

[23] V. Goiffon, P. Magnan, P. Martin-Gonthier, C. Virmontois, and M. Gaillardin, "Evidence of a novel source of random telegraph signal in CMOS image sensors," *IEEE Electron Device Lett.*, vol. 32, no. 6, pp. 773–775, Jun. 2011.

[24] C. Virmontois *et al.*, "Dark current random telegraph signals in solid-state image sensors," *IEEE Trans. Nucl. Sci.*, vol. 60, no. 6, pp. 4323–4331, Dec. 2013.

[25] T. Nuns, G. Quadri, J.-P. David, O. Gilard, and N. Boudou, "Measurements of random telegraph signal in CCDs irradiated with protons and neutrons," *IEEE Trans. Nucl. Sci.*, vol. 53, no. 4, pp. 1764–1771, Aug. 2006.

[26] A. Brunner *et al.*, "Improvement of RTS noise in HgcDTe MWIR detectors," *J. Electron. Mater.*, vol. 43, no. 8, p. 3060, 2014.

[27] D. Pogany, S. Ababou, G. Guillot, X. Hugon, B. Vilotitch, and C. Lenoble, "Study of RTS noise and excess currents in lattice-mismatched InP/InGaAs/InP photodetector arrays," *Solid-State Electron.*, vol. 38, no. 1, pp. 37–49, Jan. 1995.

[28] C. Virmontois *et al.*, "Total ionizing dose versus displacement damage dose induced dark current random telegraph signals in CMOS image sensors," *IEEE Trans. Nucl. Sci.*, vol. 58, no. 6, pp. 3085–3094, Dec. 2011.

[29] C. Virmontois *et al.*, "Displacement damage effects due to neutron and proton irradiations on CMOS image sensors manufactured in deep submicron technology," *IEEE Trans. Nucl. Sci.*, pp. 3101–3108, Dec. 2010.

[30] E. Martin, T. Nuns, C. Virmontois, J.-P. David, and O. Gilard, "Proton and γ-rays irradiation-induced dark current random telegraph signal in a 0.18-μm CMOS image sensor," *IEEE Trans. Nucl. Sci.*, vol. 60, no. 4, pp. 2503–2510, Aug. 2013.

[31] M. A. Kinch, R. L. Strong, and C. A. Schaake, "1/f noise in HgCdTe focal-plane arrays," *J. Electron. Mater.*, vol. 42, no. 11, pp. 3243–3251, Nov. 2013.

[32] A. Chantre and L. C. Kimerling, "Configurationally multistable defect in silicon," *Appl. Phys. Lett.*, vol. 48, no. 15, pp. 1000–1002, Apr. 1986.

[33] A. Jay *et al.*, "Simulation of single particle displacement damage in silicon—Part II: Generation and long-time relaxation of damage structure," *IEEE Trans. Nucl. Sci.*, vol. 64, no. 1, pp. 141–148, Jan. 2017.

[34] Y. Mori, K. Takeda, and R.-I. Yamada, "Random telegraph noise of junction leakage current in submicron devices," *J. Appl. Phys.*, vol. 107, no. 1, Jan. 2010, Art. no. 014509.